Geophysical Research Letters

RESEARCH LETTER
10.1029/2023GL102850

Clouds Increasingly Influence Arctic Sea Surface Temperatures as CO_2 Rises

A. Sledd[1,2], T. S. L'Ecuyer[3,4], J. E. Kay[1,5], and M. Steele[6]

[1]Cooperative Institute for Research in Environmental Sciences, University of Colorado Boulder, Boulder, CO, USA, [2]National Oceanic and Atmospheric Administration Physical Science Laboratories, Boulder, CO, USA, [3]Department of Atmospheric and Oceanic Sciences, University of Wisconsin-Madison, Madison, WI, USA, [4]Cooperative Institute for Meteorological Satellite Studies, Madison, WI, USA, [5]Department of Atmospheric and Oceanic Sciences, University of Colorado Boulder, Boulder, CO, USA, [6]Polar Science Center, Applied Physics Laboratory, University of Washington, Seattle, WA, USA

Abstract As Arctic sea ice retreats during the melt season, the upper ocean warms in response to atmospheric heat fluxes. Overall, clouds reduce these fluxes in summer, but how the radiative impacts of clouds on ocean warming could change as sea ice declines has not been documented. In global climate model simulations with variable CO_2, the timing of sea ice retreat strongly influences the amplitude of cloud-induced summer cooling at the ocean surface. Under pre-industrial CO_2 concentrations, summer clouds have little direct effect on maximum annual sea surface temperatures (SST). When CO_2 concentrations increase, sea ice retreats earlier, allowing more solar radiation to warm the ocean. Clouds can counteract this summer warming by reflecting solar radiation back to space. Consequently, clouds explain up to 13% more variability in maximum annual SST under modern-day CO_2 concentrations. Maximum annual SST are three times more sensitive to summer clouds when CO_2 concentrations are four times pre-industrial levels.

Plain Language Summary With higher concentrations of carbon dioxide in the atmosphere, the Arctic is warmer and has less sea ice. When sea ice melts earlier in the summer, the underlying ocean surface is exposed for longer periods of time, absorbing more energy and reaching higher temperatures. Previous studies have shown that clouds can alter the amount of energy that is absorbed at the surface, either cooling the surface by blocking incoming sunlight or warming the surface by trapping thermal energy released from the Earth. However, little work has directly linked clouds to Arctic Ocean temperatures. Using a global climate model, we investigate the relationships between clouds and ocean temperatures before and after sea ice completely melts in experiments with different carbon dioxide levels. With low levels of carbon dioxide, sea ice covers the ocean through most of the summer, and clouds have little influence on the ocean. With higher carbon dioxide levels, the ocean is free of sea ice earlier in summer when clouds have a stronger influence on how much sunlight reaches the surface. These findings suggest that when the Arctic becomes seasonally ice free, clouds will have a stronger net cooling effect on the ocean during summer.

Key Points:

- During the pre-industrial era, sea ice retreat timing, not clouds, primarily explains maximum annual Arctic sea surface temperatures (SST)
- As sea ice retreats closer to the June solstice, clouds increasingly explain maximum annual SST
- When the Arctic is seasonally ice-free, maximum SST is 3X more sensitive to clouds than in the pre-industrial era

Supporting Information:

Supporting Information may be found in the online version of this article.

Correspondence to:

A. Sledd,
anne.sledd@noaa.gov

Citation:

Sledd, A., L'Ecuyer, T. S., Kay, J. E., & Steele, M. (2023). Clouds increasingly influence Arctic sea surface temperatures as CO_2 rises. *Geophysical Research Letters*, *50*, e2023GL102850. https://doi.org/10.1029/2023GL102850

Received 8 JUL 2022
Accepted 13 APR 2023

1. Introduction

Arctic sea ice loss is occurring at unprecedented rates in all seasons (Stroeve & Notz, 2018), with cascading impacts on the rest of the Arctic system (Wood et al., 2015). As sea ice melts earlier in the summer over more area, larger regions of open ocean are exposed for longer periods of time (Stroeve et al., 2014). In turn, energy that would have otherwise contributed to melting sea ice can instead warm the upper ocean, leading to regions with sustained sea ice loss having the strongest ocean warming trends (Carvalho & Wang, 2020). As a result of warmer Arctic sea surface temperatures (SST), more heat is released from the ocean, delaying when ice starts growing (Serreze et al., 2009) and fueling an atmospheric response to sea ice loss (Manabe & Stouffer, 1980). Higher SST have further consequences for marine life (Divoky et al., 2021; Tsujii et al., 2021) and carbon uptake (DeGrandpre et al., 2020).

Given current Arctic sea ice decline and ocean warming, understanding Arctic SST is of increasing interest. Ocean temperatures in the Arctic are dominated by ocean heat convergence and ocean surface heat fluxes (Lique & Steele, 2013; Steele et al., 2010). The surface energy budget primarily determines heat uptake on a seasonal time scale because of the intense seasonality of Arctic solar insolation. Specifically, the earlier sea ice completely melts from a region the more incoming radiation can be absorbed by the ocean (Carmack et al., 2015). This

relationship is particularly important for interior Arctic seas where vertical air-sea fluxes have a larger influence on the surface energy budget than lateral advection (Carmack & Wassmann, 2006). Steele and Dickinson (2016) showed that the timing of when sea ice completely melts strongly influences annual SST maxima in the Pacific Basin of the Arctic. In observations, the dates of when sea ice begins and then completely melts are occurring earlier, on the order of 5–10 days earlier per decade (Bliss et al., 2019; Peng et al., 2018), and Arctic oceans are already absorbing more solar radiation now than in previous decades (Sledd & L'Ecuyer, 2021). These trends are predicted to continue in coming years (Crawford et al., 2021; Lebrun et al., 2019), which will further alter the surface energy balance as the ocean continues warming (Carton et al., 2015).

Despite the known importance of clouds for the Arctic energy budget, for example, Intrieri et al. (2002), Sedlar et al. (2011), and Kay and L'Ecuyer (2013), the influence of clouds on upper ocean warming has yet to be fully explored. Clouds warm the surface by trapping and re-emitting longwave (LW) radiation and cool the surface by reflecting shortwave (SW) radiation that would otherwise be absorbed (Shupe & Intrieri, 2004). Since clouds influence the surface energy balance, and the surface energy balance impacts Arctic SST, it seems reasonable to conclude that clouds could impact SST. Previous works have focused on the influence of clouds on sea ice, for example, spring melt onset (Mortin et al., 2016) and the 2007 record minima (Kay et al., 2008), but the timing of when radiative anomalies have the largest impact on SST maxima likely differs from that for sea ice due the insulating effects of sea ice on the ocean (Perovich et al., 2007). In the few studies that have considered the influences of clouds on Arctic SST, clouds were not actually the focus, so the results were either speculative based on limited data (Minnett, 1999) or only briefly mentioned using reanalysis data (Carvalho & Wang, 2020), which have known biases for Arctic clouds, for example, Lindsay et al. (2014).

In this work we investigate the extent to which clouds influence Arctic SST annual maxima using new experiments in a state of the art coupled climate model. We first ask if clouds can affect ocean surface warming in the Arctic, and, if so, is it through warming or cooling effects? Second we ask, do the impacts of clouds on SST change with a warming climate? We use model experiments with variable CO_2 concentrations to answer these questions and quantify how the sensitivity of annual SST maxima to clouds could change with rising CO_2.

2. Materials and Methods

2.1. Data

We use the Community Earth System Model version 2.1.3 (CESM2; Danabasoglu et al., 2020) for this work with the following components: Community Atmosphere Model version 6 (CAM6), Parallel Ocean Program (POP) version 2, Community Land Model (CLM) version 5.0, Los Alamos Sea Ice Model (CICE) version 5, OAA WaveWatch-III ocean surface wave prediction model (WW3), Community Ice Sheet Model (CISM) Version 2.1, and Model for Scale Adaptive River Transport (MOSART). All model simulations are fully coupled between components. The atmosphere grid has nominal resolution of $0.9 \times 1.25°$, and the ocean and ice grids have 1° resolution. Additional output was saved in each simulation from the Cloud Feedback Model Intercomparison Project Observational Simulator Package version 2.0 (COSP2; Swales et al., 2018) lidar simulator (Chepfer et al., 2008) with 250 sub-columns. This output allows scale-aware and definition-aware comparisons to monthly cloud fraction observations from CALIPSO GOCCP for June 2006 through March 2018, available up to 82°N (Chepfer et al., 2010).

We ran three simulations in CESM2 with variable CO_2 concentrations. The control run (hereafter called PI-control) uses pre-industrial forcing, nominally year 1850 with 284.7 ppm CO_2 concentration. Additional runs were branched from a separate pre-industrial run with 1% annually increasing CO_2. Branches were started after years 40 and 140, corresponding to CO_2 levels of 424.0 and 1193.3 ppm, respectively, with CO_2 levels kept constant after branching. The former run represents approximately modern-day conditions (global average CO_2 concentrations were 417.2 ppm in 2022 (Friedlingstein et al., 2022)), called CO_2-modern, and the latter is roughly four times the pre-industrial CO_2 concentration, called CO_2-high. Each simulation was run for 100 years. The annual mean temperatures over the Arctic (>60°N) are 264, 265, and 275 K for the simulations, from lowest to highest CO_2 concentrations respectively. In PI-control and CO_2-modern simulations there are small drifts in temperature (Figure S1a in Supporting Information S1). CO_2-high does not reach equilibrium in 100 years, but for the purposes of this study the CO_2-high Arctic is in a different state with respect to sea ice, clouds, and SST that still provides contrast to the lower CO_2 simulations. In particular, the Arctic is seasonally ice-free in CO_2-high (Figure S1b in Supporting Information S1).

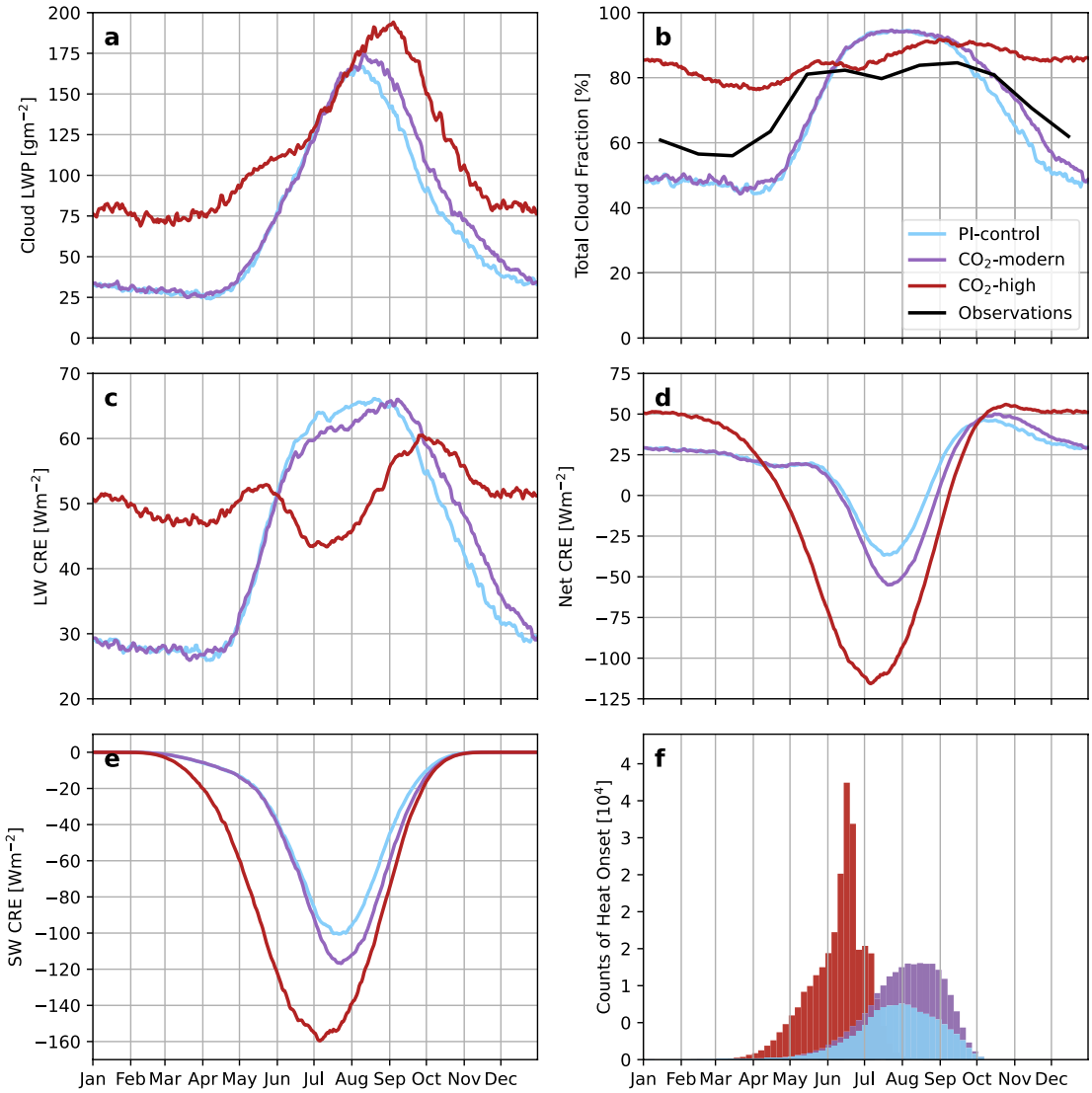

Figure 1. Annual cycles of (a) cloud liquid water path (LWP), (b) total cloud fraction (CF_{tot}), (c) LW cloud radiative effect (CRE), (d) net CRE, (e) SW CRE, and (f) histograms of heat onset. All CRE are calculated at the surface. For all CESM2 data in (a–e), only ocean grid cells poleward of 70°N are included. Observations in (b) are from CALIPSO GOCCP.

While model biases exist, CESM2 is an effective tool for investigating the changing cloud influence on Arctic SST over a large range of Arctic climates. Overall CESM2 reasonably simulates the coupled Arctic Ocean system, for example, DeRepentigny et al. (2020), DuVivier et al. (2020), and McIlhattan et al. (2020). Summer sea ice retreat is excessive when compared to modern satellite observations, but this increased summer retreat does not change the fundamental relationships identified in this work. Annual cycles of total cloud fraction (CF_{tot}) from COSP2 in PI-control and CO_2-modern simulations broadly agree with the seasonal cycle from CALIPSO GOCCP observations (Figure 1b).

2.2. Season Definitions

To study the impacts of clouds on annual maximum SST, we use several descriptive dates and time periods as defined in Steele and Dickinson (2016). The key dates for sea ice melting and upper ocean warming are determined using daily time series of sea ice concentration (SIC) and SST for individual grid boxes with a 15-day running mean boxcar smoother applied. In a given year, the day of melt onset for a grid box is defined as the last day SIC is greater than or equal to 0.95. This date is the start of the melt season. The melt season ends on the

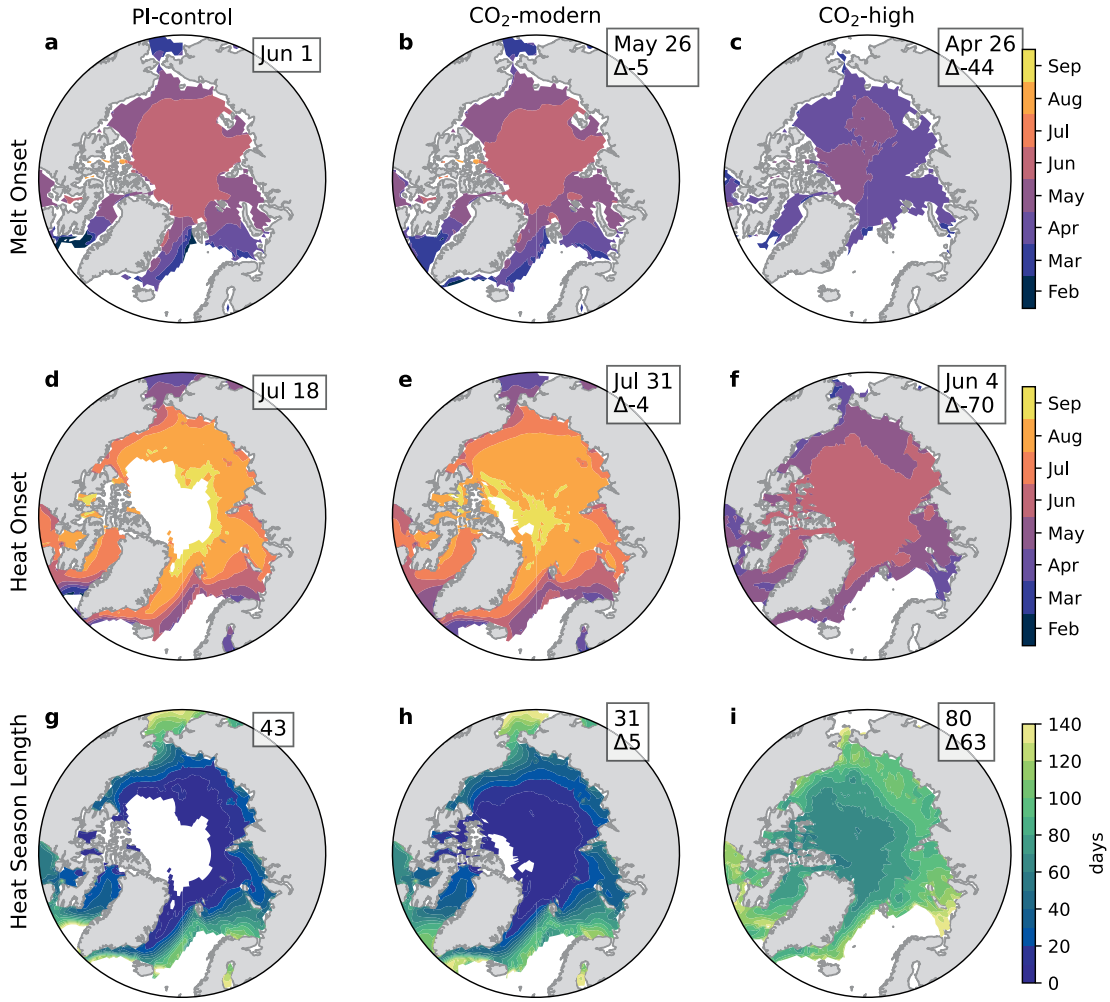

Figure 2. Average date of melt onset (a–c), heat onset (d–f) and length of heat season (g–i) from 100 year runs with different fixed CO_2 concentrations. Mean values are given in the upper right boxes of each subfigure, along with the average difference between CO_2-modern and CO_2-high experiments minus PI-control for only grid cells that experience heat and melt onset in both runs, indicated by Δ. Differences are given in days.

last day SIC is at or above 0.15, termed the day of heat onset. The heat season lasts from the day of heat onset until the day of maximum SST (SST_{max}). Defining these seasons allows for more physical comparisons than monthly lag-correlations that are often used. Additional variables, for example, total cloud fraction (CF_{tot}) and cloud liquid water path (LWP), are averaged over each season to correlate with SST_{max}. Time series are linearly de-trended prior to statistics being calculated. In addition to melt and heat seasons, we also reference meteorological summer, defined as June, July, and August.

3. Results

In PI-control, Arctic sea ice persists through most of summer (Figure 2). The mean date of melt onset occurs in April at latitudes below 70°N (exterior Arctic) and in June poleward of 70°N (interior Arctic) (Figure 2a). In the interior Arctic, heat onset typically occurs in August or September if at all (Figure 2d). While the heat season can last 3–4 months in the exterior Arctic, it lasts only ∼2 weeks on average in the interior Arctic (Figure 2g). Considering all grid cells that experience heat onset leads to an Arctic-wide average of 43 days for the heat season length.

With higher CO_2 levels, sea ice melts earlier and the ocean warms for longer. In CO_2-modern, heat onset occurs at the beginning of August in the interior Arctic, on average (Figure 2e). In this simulation, over 50% more grid cells have sea ice that completely melts, typically further north and later in the year, than in PI-control. Because more grid cells become ice free later in the year further north (Figure 2e vs. Figure 2d, Figure 1f), the date of

heat onset averaged over the entire Arctic is actually later in the year compared to PI-control (means given in Figures 2d and 2e). However, for grid cells that experience heat onset in both simulations, melt and heat onsets typically occur earlier in CO_2-modern than in PI-control (Δs in Figures 2b and 2e). The length of the heat season is also longer in CO_2-modern than in PI-control when comparing only grid cells that experience heat seasons in both simulations. The changes in heat season length are greatest around the interior Arctic coast where locally differences are on the order of a few weeks (Figure 2h vs. Figure 2g). The largest changes for these dates occur when CO_2 is quadrupled. In CO_2-high, all sea ice completely melts in summer, on average by June 4 (Figure 2f). Because much of the ocean is ice-free earlier in the year, the heat season can last up to several months even toward the North Pole in CO_2-high (Figure 2i), as compared to just a few weeks in PI-control (Figure 2g). The interannual variability of SST_{max} also increases by approximately a factor of two from PI-control to CO_2-high (not shown).

The timing of when a given area of ocean begins warming is important because the radiative effects of clouds vary throughout the year: clouds cool the surface in summer but warm the surface the rest of the year. The cloud radiative effect (CRE) is defined as the difference between all-sky and clear-sky fluxes:

$$SW_{CRE} = SW_{net,all\text{-}sky} - SW_{net,clear\text{-}sky} \quad (1)$$

$$LW_{CRE} = LW_{net,all\text{-}sky} - LW_{net,clear\text{-}sky} \quad (2)$$

$$CRE_{net} = SW_{CRE} + LW_{CRE}, \quad (3)$$

where fluxes are positive down. In PI-control and CO_2-modern clouds cool the surface (net CRE is negative) for fewer than 3 months during summer (Figure 1d). In CO_2-modern SW CRE is stronger by almost 20 Wm^{-2} in July compared to PI-control because there is less sea ice in CO_2-modern; clouds are more reflective compared to open ocean than compared to sea ice, for example, Alkama et al. (2020). During summer the warming effect of clouds is slightly reduced in CO_2-modern compared to PI-control (Figure 1c) despite similar cloud cover in these two runs (Figures 1a and 1b). Because the atmosphere is warmer with higher CO_2, clear-sky LW increases and the relative warming impact of the clouds decreases, for example, Sedlar and Devasthale (2012). Over September through December LW CRE is a few Wm^{-2} greater in CO_2-modern than in PI-control. Larger LW CRE is consistent with greater CF_{tot} and LWP compared to PI-control over the same months (Figures 1a and 1b). This increased cloud cover is also in agreement with observed fall cloud-sea ice feedbacks (Morrison et al., 2019).

These changes in CRE are amplified in CO_2-high. During June through September LW CRE is about 12 Wm^{-2} less positive than PI-control (Figure 1c), consistent with a much warmer atmosphere and greater clear-sky downwelling LW compared to lower CO_2 experiments. SW CRE is up to 60 Wm^{-2} more negative during the same months as sea ice declines (Figure 1e). SW CRE also becomes stronger before summer in CO_2-high because LWP and CF_{tot} increase in March through June compared to PI-control (Figures 1a and 1b). Greater cloud cover allows more SW to be reflected by clouds and prevented from being absorbed at the surface. Additionally, increased LWP and CF_{tot} in CO_2-high increase LW CRE from October to June by upwards of 20 Wm^{-2}. The combined impact is that net CRE is negative from May to September, meaning clouds have a larger cooling effect for longer at the surface in CO_2-high than in the lower CO_2 experiments (Figure 1d).

The earlier an ocean region begins warming, the greater the cooling effect of clouds during the heat season. As a result, in PI-control and CO_2-modern clouds cool the ocean when it is free of sea ice along the interior Arctic coasts and further south (Figure 3). In contrast, poleward from the coasts average net CRE during the heat season is positive and clouds warm the ocean. In PI-control (CO_2-modern), regions where heat onset occurs before July (Figures 2d and 2e) have more negative average net CRE, −67 (−73) Wm^{-2}, compared to grid cells that melt during or after July, −13 (−4) Wm^{-2} (Figures 3a and 3b). In CO_2-modern, 24% more grid cells experience negative net CRE during the heat season, on average, than in PI-control. This increase suggests that clouds may already be cooling the surface more in our current climate than in the pre-industrial era. Meanwhile in CO_2-high, the average heat onset occurs before July in all grid cells (Figure 2f), and the average heat season net CRE is strongly negative (Figure 3c). Not only do clouds have a net cooling effect over entire Arctic Ocean during the heat season, but the strength of the cooling effect is also greater. In CO_2-high the average net CRE is −91 Wm^{-2} during the heat season, a 34% increase compared to the lower CO_2 runs.

Despite clouds influencing surface radiation under all CO_2 concentrations, they have limited influence on SST_{max} during the heat season in PI-control and CO_2-modern. In these simulations, SST_{max} is instead strongly

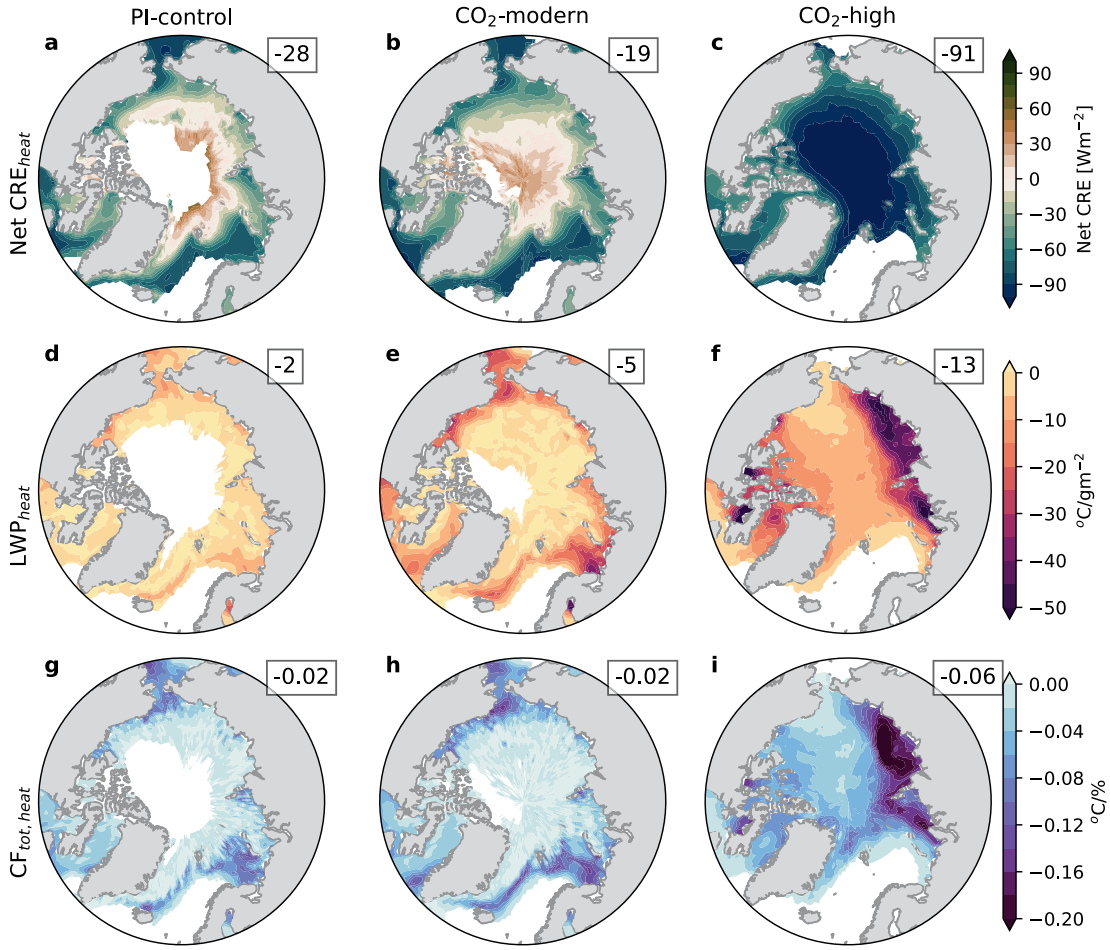

Figure 3. Average net CRE during heat season (a–c) and regressions between average heat season LWP (d–f) and total CF (g–i) and maximum annual SST for simulations with variable CO_2 concentrations. Mean values are given in upper right boxes of each subfigure.

controlled by the date of heat onset (Figures 4a and 4b). Negative correlations mean earlier heat onset leads to warmer SST_{max}. This relationship is consistent with the findings of Steele and Dickinson (2016) that earlier heat onset allows more energy to be absorbed by the ocean. Averaged over the full Arctic, heat onset explains 60% (69%) of SST_{max} variability in PI-control (CO_2-modern). Around the interior Arctic coast, average cloud LWP and CF_{tot} during the heat season (LWP_{heat}, $CF_{tot,\,heat}$) and SST_{max} have weak negative correlations in PI-control (Figures 4j and 4m), suggesting clouds have a net cooling effect on annual maximum SST, consistent with Figure 3a. Farther poleward, clouds have fewer statistically significant correlations with SST_{max} (stippling based on *t*-test with 95% confidence). The extensive sea ice in these simulations shields the ocean from the atmosphere and clouds since most incoming energy goes toward melting the sea ice.

In PI-control and CO_2-modern simulations, clouds primarily impact SST_{max} during the melt season. The melt season occurs in summer when CRE is most strongly negative. Average CF_{tot} and cloud LWP over the melt season ($CF_{tot,melt}$, LWP_{melt}) negatively correlate with SST_{max} (∼−0.5; Figures 4d, 4e, 4g, and 4h). Overall, clouds during the melt season (typically June through August) cool the surface so that it takes longer for sea ice to retreat. In turn, the longer sea ice persists in a given region, the later heat onset occurs, if at all. Because the date of heat onset is so strongly correlated to SST_{max} its delay leads to less warming.

Even increasing CO_2 from pre-industrial to present day levels leads to clouds having greater impacts on SST_{max}. In PI-control, SST_{max} is relatively insensitive to LWP and CF_{tot} during the heat season (Figures 3d and 3g). In CO_2-modern, SST_{max} is sensitive to clouds during the heat season outside of the interior Arctic basin on the order of $-15\,°C/gm^{-2}$ or $-0.1\,°C/\%$, notably north of the Atlantic Ocean, the Barents and Bering Seas, as well as the Canadian coast (Figures 3e and 3h). Clouds in these regions also explain more SST_{max} variability during the heat

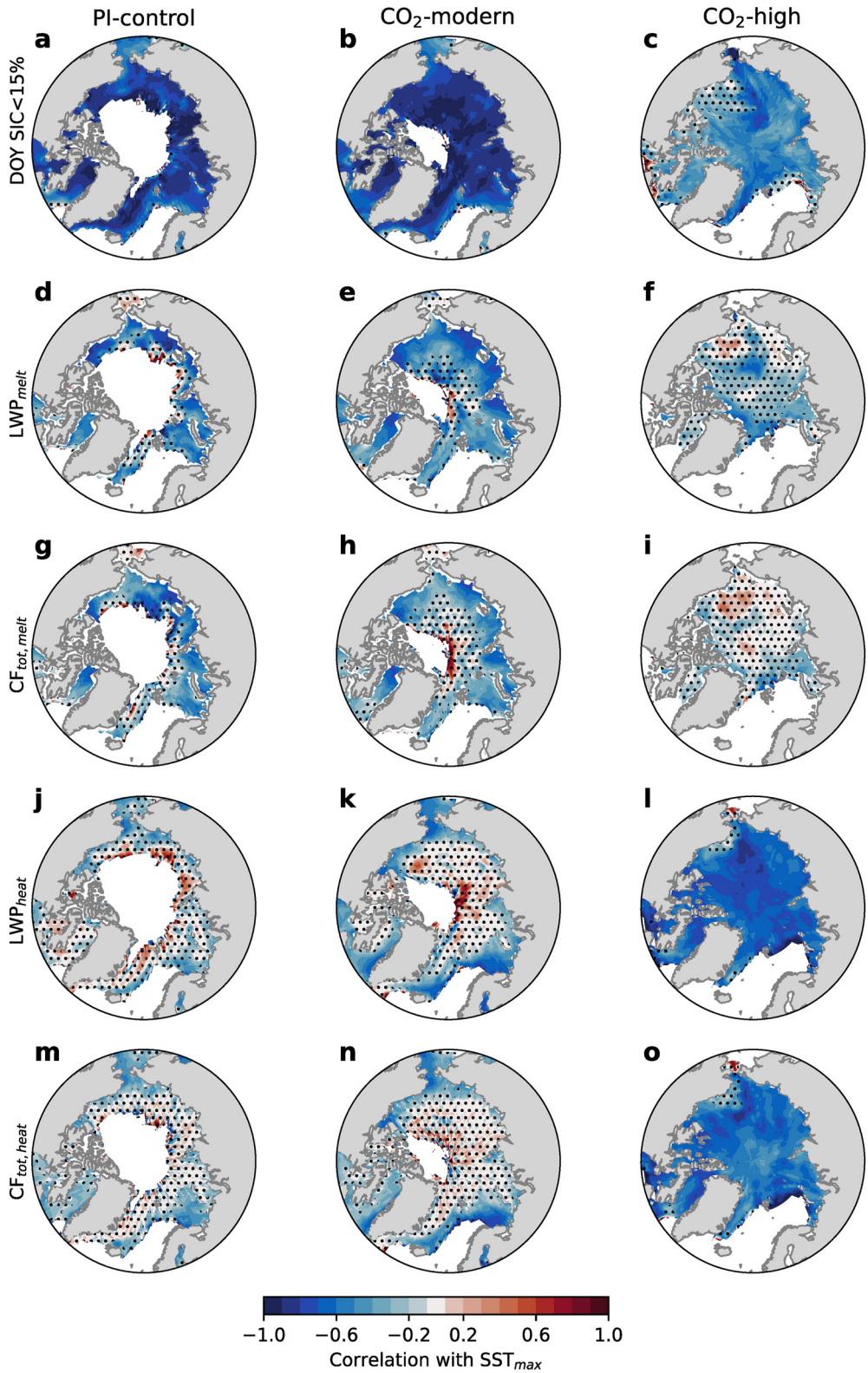

Figure 4. Correlations between variables and maximum annual SST for runs with variable CO_2. Stippling represents correlations that are not statistically significant with 95% confidence.

season in CO_2-modern than in PI-control. Correlations between LWP_{heat} and SST_{max} grow stronger, that is, more negative, most often in areas that consistently become ice free by the end of summer compared to PI-control, such as the Barents and Bering Seas (Figure 4k). Averaged over grid cells with mean heat onset dates in June or earlier (pink and purple areas in Figure 2e), LWP_{heat} explains 13% more variability in SST_{max} than in PI-control (Figure S2 in Supporting Information S1).

Notably, as CO_2 increases to levels well beyond present-day values, fundamental changes occur in the relationships between clouds, heat onset, and SST_{max}. In CO_2-high, clouds are more important to SST_{max} than the timing of heat onset (Figures 4l and 4o vs. Figure 4c), a significant shift from PI-control and CO_2-modern simulations. LWP_{heat} explains 35% more variability in SST_{max} while the date of heat onset explains 36% less variability than in PI-control (Figure S2 in Supporting Information S1). Nearly all ocean grid cells in CO_2-high completely melt before the end of June, near the summer solstice, which reduces the previously large variability of how much downwelling SW could be absorbed by the ocean based on the date of heat onset. On average, most grid cells begin warming at least a month earlier than in PI-control, closer to the time when net surface flux peaks and SW CRE is at its most negative (Figure 1e). As a result, the ocean is warming when clouds are most strongly cooling the surface.

When CO_2 is quadrupled from PI-control, the sensitivity of SST_{max} during melt and heat seasons changes in both magnitude and spatial pattern. SST_{max} in CO_2-high becomes three times more sensitive to clouds during the heat season averaged over the Arctic than in PI-control (-0.06°C/% compared to -0.02°C/%). This increased sensitivity of SST_{max} to clouds during the heat season corresponds with decreased sensitivity to clouds during the melt season (Figure S3 in Supporting Information S1). With lower CO_2 concentrations, the sensitivity of SST_{max} to clouds is largely dictated by latitude and the timing of sea ice melt; areas that melt earlier in the summer are more sensitive to clouds. In CO_2-high, SST_{max} is most sensitive to clouds north of Siberia and the Canadian Arctic Archipelago, upwards of -50°C/gm^{-2} or -0.2°C/% locally (Figures 3f and 3i). This pattern is likely because ocean surface warming on these "interior shelves" (Carmack & Wassmann, 2006) is mostly influenced by atmospheric surface heat fluxes, as opposed to northward-flowing warm currents from the North Atlantic and Pacific Oceans (e.g., Polyakov et al., 2020; Steele et al., 2010).

4. Discussion and Summary

A novel contribution of this work is quantifying the seasonal impacts of clouds on Arctic SST under increased CO_2 concentrations. We find that under PI-forcing, clouds have little impact on SST_{max}, regardless of season, because sea ice persists through summer and the underlying ocean is largely shielded from cloud radiative effects. Instead of clouds, the timing of when the ocean begins warming largely controls SST_{max}, explaining 60% of its variability. This result is consistent with observations from Steele and Dickinson (2016) that the date of sea ice retreat explains the majority of SST_{max} variability.

The most important finding of this study is that as sea ice melts earlier with higher CO_2 levels, clouds increasingly influence SST_{max}. Even with a relatively moderate increase in CO_2 to present day levels, clouds are more important to SST_{max} than during the pre-industrial climate. Clouds influence SST_{max} during the melt season by cooling the surface and delaying the start of upper ocean warming. Where sea ice retreats earlier, clouds also explain more SST_{max} variability during the heat season because the ocean warms when cloud radiative effects are most negative. In lower latitude regions that begin warming before July, cloud LWP explains 13% more SST_{max} variability. When CO_2 is quadrupled, the sensitivity of SST_{max} to summer clouds increases by a factor of three, averaged over the whole Arctic. Overall, clouds explain 35% more SST_{max} variability during the heat season than in the pre-industrial climate over the full Arctic.

In future work, observations should be used to test if the relationships between clouds and SST are currently changing in the Arctic. While reliable satellite observations of LWP are not currently available across the Arctic, cloud fraction exhibits many of the same relationships to radiative fluxes and SST_{max} as LWP, and it is available. While we might expect clouds to have similar relationships to maximum annual SST as in the simulation with modern-day CO_2 concentrations, future work could assess to what extent this relationship exists outside of a climate model. In particular, the Arctic may be experiencing the transition of clouds influencing SST_{max}, as in the CO_2-modern run, in some Arctic basins. Based on this, work we expect clouds to grow in their importance to SST as Arctic sea ice continues to decline.

Our results suggest the representation of clouds and their radiative impacts will be increasingly important for accurately modeling heat input to the upper ocean as the Arctic transitions to being seasonally ice-free. As the Arctic undergoes this transition, realistically modeling the radiative effects of clouds will likely be important not only for representing upper ocean warming but also for modeling how much heat needs to be released from the ocean to the atmosphere before sea ice can begin freezing in the fall (Deser et al., 2010; Manabe & Stouffer, 1980).

Data Availability Statement

CESM2 data used in this work are available at https://doi.org/10.5281/zenodo.7477615 and https://doi.org/10.5281/zenodo.7478423. CALIPSO GOCCP observations can be downloaded from https://climserv.ipsl.polytechnique.fr/cfmip-obs/.

Acknowledgments
This work was supported by NASA CloudSat/CALIPSO Science Team Grants 80NSSC20K0135 (AS, TSL, JEK) and 80NSSC20K0134 (MS). MS was additionally supported by NASA Grant 80NSSC20K0768, National Science Foundation Grant OPP-1751363, and Office of Naval Research Grant N00014-17-1-2545. AS was also supported in part by NOAA cooperative agreement NA22OAR4320151. JEK was also supported by NSF AGS 1554659. We acknowledge high-performance computing support from Cheyenne (https://doi.org/10.5065/D6RX99HX) provided by NCAR's Computational and Information Systems Laboratory, sponsored by the National Science Foundation.

References

Alkama, R., Taylor, P. C., Martin, G.-S., Douville, H., Duveiller, G., Forzieri, G., et al. (2020). Clouds damp the radiative impacts of polar sea ice loss. *The Cryosphere*, *14*(8), 2673–2686. https://doi.org/10.5194/tc-14-2673-2020

Bliss, A. C., Steele, M., Peng, G., Meier, W. N., & Dickinson, S. (2019). Regional variability of arctic sea ice seasonal change climate indicators from a passive microwave climate data record. *Environmental Research Letters*, *14*(4), 045003. https://doi.org/10.1088/1748-9326/aafb84

Carmack, E., Polyakov, I., Padman, L., Fer, I., Hunke, E., Hutchings, J., et al. (2015). Toward quantifying the increasing role of oceanic heat in sea ice loss in the new Arctic. *Bulletin of the American Meteorological Society*, *96*(12), 2079–2105. https://doi.org/10.1175/bams-d-13-00177.1

Carmack, E., & Wassmann, P. (2006). Food webs and physical–biological coupling on pan-arctic shelves: Unifying concepts and comprehensive perspectives. *Progress in Oceanography*, *71*(2–4), 446–477. https://doi.org/10.1016/j.pocean.2006.10.004

Carton, J. A., Ding, Y., & Arrigo, K. R. (2015). The seasonal cycle of the arctic ocean under climate change. *Geophysical Research Letters*, *42*(18), 7681–7686. https://doi.org/10.1002/2015gl064514

Carvalho, K., & Wang, S. (2020). Sea surface temperature variability in the Arctic Ocean and its marginal seas in a changing climate: Patterns and mechanisms. *Global and Planetary Change*, *193*, 103265. https://doi.org/10.1016/j.gloplacha.2020.103265

Chepfer, H., Bony, S., Winker, D., Cesana, G., Dufresne, J., Minnis, P., et al. (2010). The GCM-oriented calipso cloud product (CALIPSO-GOCCP). *Journal of Geophysical Research*, *115*(D4), D00H16. https://doi.org/10.1029/2009jd012251

Chepfer, H., Bony, S., Winker, D., Chiriaco, M., Dufresne, J.-L., & Sèze, G. (2008). Use of calipso lidar observations to evaluate the cloudiness simulated by a climate model. *Geophysical Research Letters*, *35*(15), L15704. https://doi.org/10.1029/2008gl034207

Crawford, A., Stroeve, J., Smith, A., & Jahn, A. (2021). Arctic open-water periods are projected to lengthen dramatically by 2100. *Communications Earth & Environment*, *2*(1), 1–10. https://doi.org/10.1038/s43247-021-00183-x

Danabasoglu, G., Lamarque, J.-F., Bacmeister, J., Bailey, D., DuVivier, A., Edwards, J., et al. (2020). The community Earth system model version 2 (CESM2). *Journal of Advances in Modeling Earth Systems*, *12*(2). https://doi.org/10.1029/2019ms001916

DeGrandpre, M., Evans, W., Timmermans, M.-L., Krishfield, R., Williams, B., & Steele, M. (2020). Changes in the Arctic Ocean carbon cycle with diminishing ice cover. *Geophysical Research Letters*, *47*(12), e2020GL088051. https://doi.org/10.1029/2020gl088051

DeRepentigny, P., Jahn, A., Holland, M. M., & Smith, A. (2020). Arctic sea ice in two configurations of the CESM2 during the 20th and 21st centuries. *Journal of Geophysical Research: Oceans*, *125*(9), e2020JC016133. https://doi.org/10.1029/2020jc016133

Deser, C., Tomas, R., Alexander, M., & Lawrence, D. (2010). The seasonal atmospheric response to projected arctic sea ice loss in the late twenty-first century. *Journal of Climate*, *23*(2), 333–351. https://doi.org/10.1175/2009jcli3053.1

Divoky, G., Brown, E., & Elliott, K. (2021). Reduced seasonal sea ice and increased sea surface temperature change prey and foraging behavior in an ice-obligate arctic seabird, Mandt's black guillemot (Cepphus grylle mandtii). *Polar Biology*, *44*(4), 701–715. https://doi.org/10.1007/s00300-021-02826-3

DuVivier, A. K., Holland, M. M., Kay, J. E., Tilmes, S., Gettelman, A., & Bailey, D. A. (2020). Arctic and Antarctic sea ice mean state in the community Earth system model version 2 and the influence of atmospheric chemistry. *Journal of Geophysical Research: Oceans*, *125*(8), e2019JC015934. https://doi.org/10.1029/2019jc015934

Friedlingstein, P., Jones, M. W., O'Sullivan, M., Andrew, R. M., Bakker, D. C., Hauck, J., et al. (2022). Global carbon budget 2021. *Earth System Science Data*, *14*(4), 1917–2005. https://doi.org/10.5194/essd-14-1917-2022

Intrieri, J., Fairall, C., Shupe, M., Persson, P., Andreas, E., Guest, P., & Moritz, R. (2002). An annual cycle of arctic surface cloud forcing at SHEBA. *Journal of Geophysical Research*, *107*(C10), SHE–13.

Kay, J. E., & L'Ecuyer, T. (2013). Observational constraints on Arctic Ocean clouds and radiative fluxes during the early 21st century. *Journal of Geophysical Research: Atmospheres*, *118*(13), 7219–7236. https://doi.org/10.1002/jgrd.50489

Kay, J. E., L'Ecuyer, T., Gettelman, A., Stephens, G., & O'Dell, C. (2008). The contribution of cloud and radiation anomalies to the 2007 Arctic sea ice extent minimum. *Geophysical Research Letters*, *35*(8), L08503. https://doi.org/10.1029/2008gl033451

Lebrun, M., Vancoppenolle, M., Madec, G., & Massonnet, F. (2019). Arctic sea-ice-free season projected to extend into autumn. *The Cryosphere*, *13*(1), 79–96. https://doi.org/10.5194/tc-13-79-2019

Lindsay, R., Wensnahan, M., Schweiger, A., & Zhang, J. (2014). Evaluation of seven different atmospheric reanalysis products in the arctic. *Journal of Climate*, *27*(7), 2588–2606. https://doi.org/10.1175/jcli-d-13-00014.1

Lique, C., & Steele, M. (2013). Seasonal to decadal variability of Arctic Ocean heat content: A model-based analysis and implications for autonomous observing systems. *Journal of Geophysical Research: Oceans*, *118*(4), 1673–1695. https://doi.org/10.1002/jgrc.20127

Manabe, S., & Stouffer, R. J. (1980). Sensitivity of a global climate model to an increase of CO_2 concentration in the atmosphere. *Journal of Geophysical Research*, *85*(C10), 5529–5554. https://doi.org/10.1029/jc085ic10p05529

McIlhattan, E. A., Kay, J. E., & L'Ecuyer, T. S. (2020). Arctic clouds and precipitation in the community Earth system model version 2. *Journal of Geophysical Research: Atmospheres*, *125*(22), e2020JD032521. https://doi.org/10.1029/2020jd032521

Minnett, P. J. (1999). The influence of solar zenith angle and cloud type on cloud radiative forcing at the surface in the arctic. *Journal of Climate*, *12*(1), 147–158. https://doi.org/10.1175/1520-0442-12.1.147

Morrison, A., Kay, J. E., Frey, W., Chepfer, H., & Guzman, R. (2019). Cloud response to Arctic sea ice loss and implications for future feedback in the CESM1 climate model. *Journal of Geophysical Research: Atmospheres*, *124*(2), 1003–1020. https://doi.org/10.1029/2018jd029142

Mortin, J., Svensson, G., Graversen, R. G., Kapsch, M.-L., Stroeve, J. C., & Boisvert, L. N. (2016). Melt onset over arctic sea ice controlled by atmospheric moisture transport. *Geophysical Research Letters*, *43*(12), 6636–6642. https://doi.org/10.1002/2016gl069330

Peng, G., Steele, M., Bliss, A. C., Meier, W. N., & Dickinson, S. (2018). Temporal means and variability of arctic sea ice melt and freeze season climate indicators using a satellite climate data record. *Remote Sensing*, *10*(9), 1328. https://doi.org/10.3390/rs10091328

Perovich, D. K., Light, B., Eicken, H., Jones, K. F., Runciman, K., & Nghiem, S. V. (2007). Increasing solar heating of the Arctic Ocean and adjacent seas, 1979–2005: Attribution and role in the ice-albedo feedback. *Geophysical Research Letters*, *34*(19), L19505. https://doi.org/10.1029/2007gl031480

Polyakov, I. V., Alkire, M. B., Bluhm, B. A., Brown, K. A., Carmack, E. C., Chierici, M., et al. (2020). Borealization of the arctic ocean in response to anomalous advection from sub-arctic seas. *Frontiers in Marine Science*, *7*, 491. https://doi.org/10.3389/fmars.2020.00491

Sedlar, J., & Devasthale, A. (2012). Clear-sky thermodynamic and radiative anomalies over a sea ice sensitive region of the arctic. *Journal of Geophysical Research*, *117*(D19). https://doi.org/10.1029/2012jd017754

Sedlar, J., Tjernström, M., Mauritsen, T., Shupe, M. D., Brooks, I. M., Persson, P. O. G., et al. (2011). A transitioning arctic surface energy budget: The impacts of solar zenith angle, surface albedo and cloud radiative forcing. *Climate Dynamics*, *37*(7), 1643–1660. https://doi.org/10.1007/s00382-010-0937-5

Serreze, M., Barrett, A., Stroeve, J., Kindig, D., & Holland, M. (2009). The emergence of surface-based Arctic amplification. *The Cryosphere*, *3*(1), 11–19. https://doi.org/10.5194/tc-3-11-2009

Shupe, M. D., & Intrieri, J. M. (2004). Cloud radiative forcing of the Arctic surface: The influence of cloud properties, surface albedo, and solar zenith angle. *Journal of Climate*, *17*(3), 616–628. https://doi.org/10.1175/1520-0442(2004)017<0616:crfota>2.0.co;2

Sledd, A., & L'Ecuyer, T. (2021). Emerging trends in arctic solar absorption. *Geophysical Research Letters*, *48*(24), e2021GL095813. https://doi.org/10.1029/2021gl095813

Steele, M., & Dickinson, S. (2016). The phenology of Arctic Ocean surface warming. *Journal of Geophysical Research: Oceans*, *121*(9), 6847–6861. https://doi.org/10.1002/2016jc012089

Steele, M., Zhang, J., & Ermold, W. (2010). Mechanisms of summertime upper Arctic Ocean warming and the effect on sea ice melt. *Journal of Geophysical Research*, *115*(C11), C11004. https://doi.org/10.1029/2009jc005849

Stroeve, J., Markus, T., Boisvert, L., Miller, J., & Barrett, A. (2014). Changes in arctic melt season and implications for sea ice loss. *Geophysical Research Letters*, *41*(4), 1216–1225. https://doi.org/10.1002/2013gl058951

Stroeve, J., & Notz, D. (2018). Changing state of arctic sea ice across all seasons. *Environmental Research Letters*, *13*(10), 103001. https://doi.org/10.1088/1748-9326/aade56

Swales, D. J., Pincus, R., & Bodas-Salcedo, A. (2018). The cloud feedback model intercomparison project observational simulator package: Version 2. *Geoscientific Model Development*, *11*(1), 77–81. https://doi.org/10.5194/gmd-11-77-2018

Tsujii, K., Otsuki, M., Akamatsu, T., Amakasu, K., Kitamura, M., Kikuchi, T., et al. (2021). Annual variation of oceanographic conditions changed migration timing of bowhead whales *Balaena mysticetus* in the southern Chukchi Sea. *Polar Biology*, *44*(12), 2289–2298. https://doi.org/10.1007/s00300-021-02960-y

Wood, K. R., Bond, N. A., Danielson, S. L., Overland, J. E., Salo, S. A., Stabeno, P. J., & Whitefield, J. (2015). A decade of environmental change in the Pacific arctic region. *Progress in Oceanography*, *136*, 12–31. https://doi.org/10.1016/j.pocean.2015.05.005